Age-related reduction in frequency-following responses as a potential marker of cochlear neural degeneration

Märcher-Rørsted, Jonatan; Encina-Llamas, Gerard; Dau, Torsten; Liberman, M. Charles; Wu, Pei zhe; Hjortkjær, Jens

Published in:
Hearing Research

Link to article, DOI:
10.1016/j.heares.2021.108411

Publication date:
2022

Document Version
Publisher's PDF, also known as Version of record

Hearing Research 414 (2022) 108411

Contents lists available at ScienceDirect

Hearing Research

journal homepage: www.elsevier.com/locate/heares

Age-related reduction in frequency-following responses as a potential marker of cochlear neural degeneration

Jonatan Märcher-Rørsted[a], Gerard Encina-Llamas[a], Torsten Dau[a], M. Charles Liberman[c], Pei-zhe Wu[c], Jens Hjortkjær[a,b,*]

[a] Hearing Systems Section, Department of Health Technology, Technical University of Denmark, Ørsteds Plads, Building 352, DK-2800 Kgs. Lyngby, Denmark
[b] Danish Research Centre for Magnetic Resonance, Centre for Functional and Diagnostic Imaging and Research, Copenhagen University Hospital Hvidovre, Kettegård Allé 30, DK-2650 Hvidovre, Denmark
[c] Eaton-Peabody Laboratories and Department of Otolaryngology, Head and Neck Surgery, Massachusetts Eye and Ear, Boston, MA 02114 USA

ARTICLE INFO

Article history:
Received 31 March 2021
Revised 3 December 2021
Accepted 6 December 2021
Available online 7 December 2021

Keywords:
Aging
Frequency-following response
Auditory nerve
Neural degeneration
Auditory nerve modeling

ABSTRACT

Healthy aging may be associated with neural degeneration in the cochlea even before clinical hearing loss emerges. Reduction in frequency-following responses (FFRs) to tonal carriers in older clinically normal-hearing listeners has previously been reported, and has been argued to reflect an age-dependent decline in temporal processing in the central auditory system. Alternatively, age-dependent loss of auditory nerve fibers (ANFs) may have little effect on audiometric sensitivity and yet compromise the precision of neural phase-locking relying on joint activity across populations of fibers. This peripheral loss may, in turn, contribute to reduced neural synchrony in the brainstem as reflected in the FFR. Here, we combined human electrophysiology and auditory nerve (AN) modeling to investigate whether age-related changes in the FFR would be consistent with peripheral neural degeneration. FFRs elicited by pure tones and frequency sweeps at carrier frequencies between 200 and 1200 Hz were obtained in older (ages 48–76) and younger (ages 20–30) listeners, both groups having clinically normal audiometric thresholds up to 6 kHz. The same stimuli were presented to a computational model of the AN in which age-related loss of hair cells or ANFs was modelled using human histopathological data. In the older human listeners, the measured FFRs to both sweeps and pure tones were found to be reduced across the carrier frequencies examined. These FFR reductions were consistent with model simulations of age-related ANF loss. In model simulations, the phase-locked response produced by the population of remaining fibers decreased proportionally with increasing loss of the ANFs. Basal-turn loss of inner hair cells also reduced synchronous activity at lower frequencies, albeit to a lesser degree. Model simulations of age-related threshold elevation further indicated that outer hair cell dysfunction had no negative effect on phase-locked AN responses. These results are consistent with a peripheral source of the FFR reductions observed in older normal-hearing listeners, and indicate that FFRs at lower carrier frequencies may potentially be a sensitive marker of peripheral neural degeneration.

1. Introduction

Aging is often accompanied by listening difficulties in noisy situations, even when audiometric thresholds indicate normal hearing (Humes, 2005). Such difficulties could be due to age-related declines in temporal processing arising at different levels of the auditory system. A number of studies have reported an age-related reduction in frequency-following responses (FFRs) to pure tones (Marmel et al., 2013) or vowels (Anderson et al., 2012; Bidelman et al., 2014; Skoe et al., 2015), also in older listeners with clinically normal audiometric thresholds (Clinard et al., 2010; Clinard and Cotter, 2015; Clinard and Tremblay, 2013; Mamo et al., 2016; Presacco et al., 2019; Roque et al., 2019). Reduced FFRs in older listeners without loss of audiometric sensitivity have been argued to reflect a decline in neural synchrony arising in the central auditory system (Anderson et al., 2012; Clinard and Cotter, 2015; Walton, 2010). Such central desynchronization has been hypothesized to cause temporal processing deficits and underlie declines in speech perception in older listeners, even in the absence of peripheral dysfunction assessed through audiometric thresholds (Frisina and Frisina, 1997; Pichora-Fuller et al., 2007). However,

* Corresponding author.
E-mail address: jhjort@dtu.dk (J. Hjortkjær).

https://doi.org/10.1016/j.heares.2021.108411

normal audiograms do not preclude a peripheral source of age-related changes in the FFR. In particular, an age-dependent degeneration of auditory nerve (AN) fibers may have little effect on audiometric thresholds (Kujawa and Liberman, 2009; Schuknecht and Woellner, 1955; Wu et al., 2020) and yet may reduce precise population-level neural phase-locking as reflected in the FFR. The current study investigates this possibility.

FFRs are neurophonic potentials generated by periodic or near-periodic auditory stimuli. The FFR reflects sustained neural activity integrated over a population of neural elements. It is often phase-locked to the individual cycles of the stimulus waveform and/or the envelope of the periodic stimuli.[1] Scalp-recorded FFRs are considered to be predominantly produced by synchronous neural activity in the rostral brainstem and midbrain (Krishnan, 2006; Marsh et al., 1974; Smith et al., 1975; Worden and Marsh, 1968). While the main generator of the scalp-recorded FFR is not peripheral (Sohmer et al., 1977), temporal coding of spectral information is first represented by neural phase-locking across populations of auditory nerve (AN) fibers (Reale and Geisler, 1980; Sachs et al., 1983; Young and Sachs, 1979). The auditory nerve neurophonic (ANN) response is the mass potential correlate of phase-locked neural activity across AN fibers recorded near the cochlea, which can be dissociated from the cochlear microphonic (CM) response produced by hair cell activity (Fontenot et al., 2017; Snyder and Schreiner, 1984; Verschooten and Joris, 2014). The ANN shows properties that reflect neural coding not present in the CM, such as rectification and adaptation (e.g., Verschooten and Joris 2014), and these response properties are also present in the scalp FFR (Snyder and Schreiner, 1985). Damage to AN fiber terminals or a suppressed spike generation in the AN abolish both the ANN and the scalp FFR (Fontenot et al., 2017; Henry, 1995; Snyder and Schreiner, 1984). Intact phase-locked activity across populations of AN fibers is thus a prerequisite for the generation of the FFR. While ANF loss diminishes or eliminates the FFR, more systematic studies of the effects of AN neuropathy on scalp FFRs are missing. It is therefore unclear whether response properties of a pathological ANN are inherited at the brainstem as reflected by the FFR.

In the present study, we propose that age-related reductions in the FFR could, at least in part, reflect the age-dependent neural degeneration in the cochlea. Synapses between inner hair cells (IHC) and AN fibers, and eventually the fibers themselves, degenerate progressively with age (Keithley et al., 1989; Sergeyenko et al., 2013). Exposure to noise accelerates this age-related cochlear synaptopathy (CS) (Fernandez et al., 2015). Recent histopathological examinations of 'normal-aging' human temporal bones have indicated an age-related AN peripheral axon loss across the cochlea (Wu et al., 2019) that typically exceeds age-related degeneration of hair cells. Such primary neural degeneration challenges the conventional understanding that outer hair cells (OHC) represent the primary and most vulnerable element in age-related hearing loss. AN fiber loss can occur without affecting audiometric thresholds, as long as the OHCs are intact (Schuknecht and Woellner, 1955).

Importantly, the degeneration of AN fibers in the aging human cochlea occurs across the cochlear partition (Viana et al., 2015; Gleich et al., 2016; Fu et al., 2019; Wu et al., 2020). A wide-spread neural loss across characteristic frequency (CF) regions in the cochlea would be expected to reduce phase-locking by AN fiber populations at both higher and lower carrier frequencies Henry (1995). Assuming that the frequency-specific response properties are preserved in the scalp-recorded FFR, the FFR would be reduced at both higher and lower carrier-tone frequencies due to fewer contributing fibers. An age-dependent decline in temporal resolution, on the other hand, should predominantly limit phase-locking at higher carrier frequencies, and thus mainly reduce FFRs at higher stimulation rates (Anderson et al., 2012; Frisina and Frisina, 1997).

Previous results are unclear as to whether an age-dependent reduction in the FFR to tonal carriers is broadly distributed across stimulation frequency. Clinard et al. (2010) reported a correlation between age and FFR amplitudes to tone frequencies around 1000 Hz, but not to lower frequency tones around 500 Hz. Using tonal frequency sweeps, Clinard and Cotter (2015) reported reduced FFRs also at lower frequencies in older listeners with normal audiometric thresholds up to 4 kHz, and also reported weaker FFRs for faster sweep rates. The authors concluded that the results reflect an age-related decline of phase-locking specific to stimuli with dynamic frequency content such as tonal sweeps. Age-dependent reductions in FFRs elicited by vowel sounds that also have dynamic frequency content (Anderson et al., 2012; Clinard and Tremblay, 2013; Presacco et al., 2019; Roque et al., 2019) may support this view. Yet, it remains unclear whether age-group effects would also be observed for tonal stimuli at lower frequencies.

Using both pure-tone stimuli and frequency sweeps, the current study investigated FFRs at different stimulation frequencies in young and older listeners with clinically normal audiograms up to 6 kHz. We hypothesized that age-related peripheral neural degeneration across the cochlea would be consistent with reduced FFR amplitudes across a range of stimulation frequencies. In addition to FFRs, we measured middle-ear muscle reflexes (MEMRs) and audiometric thresholds at extended high frequencies, each of which have been proposed to be sensitive to cochlear neurodegeneration (Valero et al., 2016; Bharadwaj et al., 2019; Liberman et al., 2016). To investigate the effects of nerve fiber loss on phase-locked responses at the level of the AN, we used a computational model of the AN (Bruce et al., 2018). Histological data from a recent human otopathologic study (Wu et al., 2020) were included to simulate the effects on the phase-locked population response. Specifically, we asked if ANF loss simulates a change in FFR that is qualitatively consistent with changes in the observed far-field FFR in aging listeners. The model was also used to dissociate the effects of neural loss from OHC damage based on age-specific threshold curves.

2. Materials and methods

2.1. Participants

Twenty-five subjects participated in the study. The participants were recruited based on standard audiometric pure-tone sensitivity profiles ($\leq$ 20 dB hearing level (HL) from 125 Hz to 6 kHz) in our patient database, and grouped by age. To ensure the validity of the audiometric data from the database, all participants took part in a clinical evaluation of their hearing status on the day of the experiment. This included audiogram measurements using Sennheiser HAD300 earphones (air conduction thresholds at audiometric frequencies 0.25, 0.5, 1, 2, 3, 4, 6 and 8 kHz, as well as for extended high-frequencies at 10, 11.25, 14 and 16 kHz), the examination of middle- and outer-ear functionality via wide-band tympanography, and otoscopy. One of the twenty-five participants was found to have slightly elevated thresholds at 3 kHz (35 dB HL) and 6 kHz (40 dB HL) and was therefore excluded from the analyses, resulting in a young group (n = 12, 5 males, mean age 24.8 +/- 3.38) and an older group (n = 12, 4 males, mean age 63.3 +/- 8.91; age difference: $t(22) = -14.01$, $p < 0.001$). All subjects provided written informed consent to participate. The experiment was approved by the Science Ethics Committee for the Capital region of Denmark (protocol H-16,036,391) and was conducted in accordance with the Declaration of Helsinki.

[1] Here, the term FFR is used to refer to the response to pure tones or tonal sweeps, as distinct from envelope-following responses (EFRs) in the case of amplitude modulated stimuli.

2.2. Distortion product optoacoustic emissions (DPOAEs)

It is possible that OHC dysfunction can confound potential differences in FFR between young and older listeners. As a physiological indicator of OHC status, distortion product otoacoustic emissions (DPOAE) were measured, both as a function of frequency (2–8 kHz at 64 dB sound pressure level (SPL)) and level (40–70 dB SPL at 4 kHz). Both negative and positive middle-ear pressure can impact the quality of DPOAE recordings (Sun, 2012). To compensate for this, we pressurized the ear to correct for middle-ear pressure while measuring DPOAEs. DPOAE measures were conducted in both ears of all participants using the Interacoustics Titan system and standardized protocols. DPOAEs were measured using two pure tones, known as primaries (F_1 and F_2) with a ratio of 1.22 (F_2/F_1). For the level dependent DPOAEs at 4 kHz, the level difference between the two primary tones was kept constant ($F_2 = F_1 - 10$ dB) while F_1 was varied in level from 40 to 70 dB SPL in steps of 10 dB. Level dependent distortion products were considered significant if their amplitude exceeded −15 dB SPL. For the frequency dependent DPOAEs, the levels of the two tones were fixed (F_1 = 65 dB SPL, and F_2 = 55 dB SPL) while the frequency of F_2 was varied (2, 3, 4, 5, 6 and 8 kHz). Cubic distortion products ($2F_1$-F_2) were recorded. Frequency dependent distortion products were considered significant if their amplitude exceeded −10 dB SPL.

2.3. Middle-ear muscle reflex

The middle-ear muscle reflex (MEMR) was measured to indicate the status of efferent neural feedback which has also been proposed to indicate potential degeneration in the auditory nerve (Bharadwaj et al., 2019; Valero et al., 2016). A custom assay was implemented according to a recent study (Mepani et al., 2019), using the Titan system. The protocol consisted of click-noise-click sequences, presented to the right ear. The click response of the ear canal was measured before and after 500 ms white noise elicitors (0.5–2 kHz) at levels of 75–105 dB SPL, using a 5 dB step size. The probe click was presented at 100 dB SPL, calibrated to the peak-to-peak voltage of a 100 dB SPL 1 kHz tone. The noise elicitors had a 50 sample (2.3 ms) long onset and offset ramp defined by a 1st order Kaiser window function. The MEMR was assessed by comparing the frequency response of the first and second click for each of the noise elicitor levels. Growth-level functions for each participant were evaluated by taking the absolute value of the frequency response differences summed across all frequencies. To investigate the sensitivity of the MEMR to different elicitor levels, a linear function was fitted to the MEMR responses. The estimated linear coefficient from the linear fit for each participant was used for the group based analysis. For one older participant, it was not possible to complete the MEMR measurement due to technical issues. Data from this participant were therefore excluded from this part of the analysis.

2.4. EEG

2.4.1. Experiment & stimuli

FFRs were recorded with both amplitude modulated pure-tones and frequency sweeps. Pure-tone stimulation consisted of continuous tones at carrier frequencies of 326 Hz and 706 Hz, sinusoidally amplitude modulated at 4 Hz. Pure-tone sequences were presented to the right ear. A total of 8 conditions of 250-s each was measured in this part of the experiment. The conditions consisted of either high or low carrier frequencies (326 and 706 Hz), alternating polarities (condensation and rarefaction start phase), as well as with or without the presence of a contralateral threshold equalizing noise (TEN) masker at a signal-to-noise ratio (SNR) of 5 dB relative to the pure-tone stimulus. Contralateral noise was presented to investigate effects of efferent feedback on the FFR. The presentation order of the conditions was randomized for each participant. Next, the participants listened to 1800 repetitions of pure-tone frequency sweeps. The stimuli consisted of 0.6 s long up-down cosine frequency-modulated sweeps ranging from 0.2 to 1.2 kHz presented continuously. The average absolute frequency change rate was of 3333 Hz/s. Due to the sinusoidal modulator, the frequency change rate was not constant across the frequency range. The onset polarity was positive and sweeps were presented in a continuous manner. The sweep stimuli were presented monaurally to the right ear for all participants. The TEN was presented to the left ear. Both pure-tone and sweep stimuli were presented via metal-shielded ER-3 insert earphones (Etymotic Research) at 85 dB HL for all conditions, synthesized at a sampling rate of 48 kHz. Preliminary measurements using dummy head recordings were conducted to ensure the absence of electrical artefacts. For the sweep and pure-tone stimuli, the level was adjusted using frequency dependent filters according to equal-loudness level contours as described in ISO 226:2003. The frequency response of the sound reproduction chain (i.e., soundcard and earphones) was linearized by means of the inverse impulse response of the earphones.

2.4.2. Data acquisition

EEG data were continuously recorded using the BioSemi ActiveTwo system. EEG was recorded from gold-foil tiptrode electrodes inside left and right ear canals, as well as from 8 pin-type scalp electrodes (CMS, DRL, Cz, FCz, Fz, Fpz, P9 and P10). The sample rate was 16,384 Hz. The participants were asked to lie down on a bed in a doubled-walled sound treated electromagnetically shielded booth, keeping their eyes closed. Otoscopy was performed directly before insertion of the tiptrodes, ensuring correct insertion. No preparation of the ear canals was performed.

2.4.3. EEG pre-processing

All EEG data were segmented into trials from 0.1 s preceding the onset of each stimulation cycle, to 0.8 s after. Line noise (50 Hz) was removed using notch filters centered around 50 Hz and the corresponding harmonics (100, 150 etc.) up to 1 kHz. The data were bandpass filtered between 80 Hz and 2 kHz using a windowed sinc type I linear phase finite impulse response filter. The data were re-referenced to the response of the right tiptrode.

2.4.4. Sweep FFR analysis

Frequency sweeps were evaluated as a combination of both horizontal and vertical montages, by using potentials from the vertex (Cz) and the left tiptrode, referenced to the right tiptrode. In this way, sources from the lower- as well as higher brainstem could contribute to the FFR to sweeps Bidelman (2018). Trials of 600 ms (corresponding to one cosine sweep cycle) were first examined for artefacts, rejecting any trials where EEG activity exceeded +/- 40 mV. Clean trials were then weighted by the inverse of their variance and averaged (John et al., 2001). On average, 3.1% +/- 4.9% of trials were rejected for this part of the analysis, leaving, on average, 1744 trials for each participant. Time frequency representations of the neural response were calculated using a discrete Gabor transform for real-signals using two-sample second-order Gaussian filters. To investigate potential differences between older and younger listeners across the entire stimulus frequency range, a stimulus-response cross-correlation analysis was performed on the average time series for each listener. This was done over the entire time course of the stimulus. To identify potential frequency dependent differences across listener groups, the instantaneous FFR over sweep frequency was calculated in the spectrotemporal domain. Time-frequency bins containing the stimulus were identified and the FFR magnitude across frequency was extracted.

2.4.5. Pure-tone FFR analysis

To evaluate the neural synchronization of the response to the tonal carrier frequency of the amplitude modulated stimuli, horizontal and vertical montages were combined using potentials from the vertex (Cz) and the left tiptrode, referenced to the right tiptrode. Trials of 0.5-s were first examined for artefacts, rejecting trials where EEG activity exceeded +/- 40 mV. On average, 1.0% +/- 2.2% of trials were rejected. Trials of negative polarities were multiplied by −1 to enhance the FFR response ((C-R)/2) (Kraus and Skoe, 2010). Clean trials were then averaged and weighted by the inverse of their variance, and concatenated to create 1-s long segments (corresponding to 2 trials of 0.5 s). FFR magnitudes were evaluated on the averaged response for each condition, and for each participant separately. The spectral magnitude at the carrier frequency (326 Hz or 706 Hz) was evaluated, and compared to the surrounding noise floor (+/- 20 Hz) using an F-statistic test (Dobie and Wilson, 1996). The SNR (F-ratio) was calculated as the power in the FFR frequency bin divided by the average of the surrounding noise floor power. Side bands from the amplitude modulation were disregarded as part of the noise floor (+/- 4 Hz around the carrier frequency). The probability (p) of the FFR power being different from the noise was assed as 1-F, where F represents the cumulative distribution of the power ratio. FFR measurements were considered statistically significant if $p \leq 0.01$ ($\alpha = 0.01$). Non-significant FFR responses were excluded from statistical analysis.

To compare the data with those from previous studies, the FFR was also analyzed using other metrics. A stimulus-response cross-correlation analysis was performed as in Clinard et al. (2010) and Marmel et al. (2013), whereby average responses were cross-correlated with a down-sampled version of the stimulus to match the EEG sample rate. The cross-correlation coefficient was chosen as the maximum value of the cross-correlation function within a time window of +/−15 ms from $t = 0$.

2.5. Auditory nerve modeling

A humanized phenomenological model of the AN (Bruce et al., 2018) was used to investigate the consequences of hair-cell and neural loss with advancing age on FFRs at the level of the nerve. The input to the model is an instantaneous pressure waveform of the stimulus and the output is a series of AN spike times. The model consists of a middle-ear filter, a nonlinear basilar membrane filtering stage mimicking OHC gain, IHC transduction, adaptation at the IHC-AN synapse, and generation of the instantaneous discharge rate. The model was implemented to simulate the whole AN population response, as in Encina-Llamas et al. (2021). In short, 32,000 AN fibers, distributed non-uniformly across 300 CFs ranging from 125 Hz to 20 kHz, were computed in each simulation. For each CF, a distribution of respectively 61%, 23% and 16% of high-, medium-, and low-SR fibers, was used (Liberman, 1978).

Histopathological data from 120 human temporal bones (Wu et al., 2020) were used to simulate plausible age-related degeneration of hair cells and ANFs in humans. The histological data consisted of microscopic analyses of hair cells, ANFs and strial tissue in 120 human inner ears. The specimens ranged in age from 0 to 104 years. Mean loss profiles of IHCs, and ANFs were evaluated in three age groups (1–50, 50–75 year and 75–100 years of age) across discrete cochlear segments (CFs 170 Hz, 300 Hz, 700 Hz, 1.8 kHz, and 7.5 kHz for ANFs, and 144 Hz, 275 Hz, 488 Hz, 832 Hz, 1391 Hz, 2297 Hz, 3767 Hz, 6150 Hz, 10,016 Hz, and 16,285 Hz for IHCs). For each CF, loss of ANFs was implemented by removing the number of fibers corresponding to the percentage loss, agnostic to fiber type (Suthakar and Liberman, 2021). In histopathological counting, IHC loss indicates loss of the whole cell (in contrast to IHC dysfunction). IHC loss was simulated by removing all ANFs connected to the missing IHC. It was then assumed that the surviving IHCs were functionally intact (i.e. the 'cihc' parameter in the model by Bruce et al. (2018) was not modified).

Directly linking OHC loss from the histopathological data to the model parameter that controls the OHC gain ('cohc' in Bruce et al. (2018)) is challenging. Instead, OHC gain loss was simulated based on audiometric thresholds by means of the MATLAB function *fitaudiogram2* implemented by Zilany et al. (2009). This adjusts the AN model thresholds to account for the audiometric threshold elevations. This was first done for standard clinical frequencies (<8 kHz) for the histopathological data of Wu et al. (2020). In addition, age-normal audiometric profiles (Rodríguez Valiente et al., 2014), also including extended high frequencies (0.125 to 20 kHz), were also simulated. This dataset is based on 635 'normal-aging' listeners between 5 and 90 years of age, grouped in 6 age groups (20–29, 30–39, 40–49, 50–59, 60–69 and 70–90 years). The mean threshold curves for each age group were used.

The same sweep stimulus and amplitude modulated pure-tones stimuli as used in the FFR experiments were used in the model simulations. The gross AN response was obtained by summing the output spike trains from each CF in the frequency domain. This avoided potential phase interaction effects induced by non-uniform nerve fiber loss across frequency, which were highly non-linear and difficult to interpret. Specifically, the 300 CFs were divided into 10 cochlear regions (CR) and the same spectral analysis was performed per CR as performed on the FFR data. Although it is known that phase interactions between basal and apical neural generator are important when interpreting transient evoked auditory brain stem responses (ABR) (Abdala and Folsom, 1995), it is still unknown to which degree these interactions influence the response to sustained frequency-dynamic stimuli, such as the sweep stimulus used in this study. It has been argued that the FFR is predominately generated by basal fibers (Dau, 2003), which might argue for only including basal fibers in the model output. Including only basal AN fibers in the model simulations led to very similar results (not shown) to the results obtained after disregarding the phase. However, due to the low-frequency content of the stimulus, and missing knowledge about the model's ability to represent phase information with complex stimuli, it was decided to include low-frequency fibers, but to disregard any phase interactions between basal and apical cochlear channels. To quantify effects of OHC dysfunction, IHC deafferentation and ANF loss, the outputs of the impaired models were normalized to the output of the 'healthy' AN model.

2.6. Statistical tests

Non-parametric permutation tests were used to examine differences between groups. To test for statistical group differences in the FFR amplitudes at different sweep frequencies, the p-values across frequency were corrected by means of false discovery rate (Benjamini and Hochberg 1995). All statistical tests were considered significant at $p < 0.05$. Permutation tests were conducted with 100,000 permutations, unless otherwise stated.

3. Results

3.1. Hearing thresholds and OAEs

We recruited younger and older listeners from our database to have normal hearing as defined by their audiometric thresholds at standard clinical frequencies up to 6 kHz. Fig. 1A) shows the measured group-averaged threshold functions (right ear) for the younger (solid black) and the older (solid red) listener groups. All listeners were confirmed to have audiometric thresholds ≤

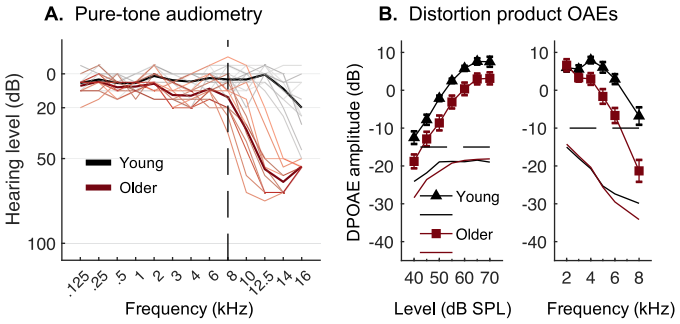

Fig. 1. A) Pure-tone audiograms from 125 Hz to 16 kHz. Individual threshold function are plotted as thin black (young) and red (older) lines. B) DPOAEs at 4 kHz for levels 40 to 70 dB SPL (left), and DPOAE grams at 64 dB SPL for frequencies 2, 3, 4, 5, 6 and 8 kHz (right). Solid lines without markers indicate the averaged noise floor. Dashed lines indicate threshold for significant responses above the noise floor. Error bars show standard error of the mean (SEM).

20 dB HL up to 6 kHz. At 8 kHz, the older listeners had thresholds $\leq$ 35 dB HL. Despite normal or near-normal audiometric thresholds in the clinical range, the older listeners had significantly higher thresholds above 8 kHz compared to the younger listeners (pure-tone average of all frequencies from 10 kHz to 16 kHz: $t(22) = -11.2396$, $p < 0.001$). Also at frequencies $\leq$ 6 kHz, the young group had significantly lower mean thresholds compared to the older group (pure-tone average from 125 to 6000 Hz: $t(22) = -4.0814$, $p < 0.001$), although both were within the normal range. There were no differences in thresholds in the frequency range of the tonal stimuli (200–1200 Hz) used in the EEG study (pure tone average from 125 to 2000 Hz: $t(22) = -1.9225$, $p = 0.0784$).

Cubic DPOAEs were measured as a correlate of OHC function. Fig. 1B) shows the group-averaged DPOAEs obtained for $F_2 = 4$ kHz as a function of *F2* level (left) and obtained for a fixed level ($F_1 = 65$ dB SPL, $F_2 = 55$ dB SPL) as a function of F_2 frequency (right). On average, significant DPOAEs were obtained for levels above 40 dB SPL in the young listeners and above 45 dB SPL in the older listeners. When averaging across level, the older listeners showed lower DPOAE responses compared to the young listeners ($t(22) = 3.2201$, $p = 0.0042$), indicating reduced OHC function in the older listeners at this frequency (4 kHz). The DPOAE frequency functions (right) showed, on average, significant DPOAEs at all frequencies in the young group. For the older group, significant DPOAEs were obtained only up to 6 kHz, and the response amplitudes were smaller than those for the young group at frequencies at and above 4 kHz, indicating decreased OHC function at the higher frequencies. Statistical analysis showed no difference between the groups at frequencies below 4 kHz (Bonferroni corrected $p < 0.0083$: 2 kHz: $t(22) = 2.4156$, $p = 0.7628$, 3 kHz: $t(22) = -0.3090$, $p = 0.1452$, 4 kHz: $t(22) = 1.5003$, $p = 0.0129$). For frequencies above 4 kHz, the older listeners showed reduced DPOAE responses compared to the young group (Bonferroni corrected $p < 0.0083$: 5 kHz: $t(22) = 3.0789$, $p = 0.0030$, 6 kHz: $t(22) = 3.8611$, $p = 0.0006$, 8 kHz: $t(22) = 3.7450$, $p = 0.0012$), consistent with elevated audiometric thresholds at higher frequencies in the older group.

3.2. Effects of age on MEMR sensitivity

Fig. 2 shows the MEMR results obtained in the two listener groups for different levels of the wide-band noise elicitor. Fig. 2A) shows the group average MEMR as a function of frequency for the younger group (left) and the older group (right). The responses represent the change in absorbance in the ear canal after the presentation of the noise elicitor. Different colors indicate the results for the different noise elicitor levels (between 75 and 105 dB SPL).

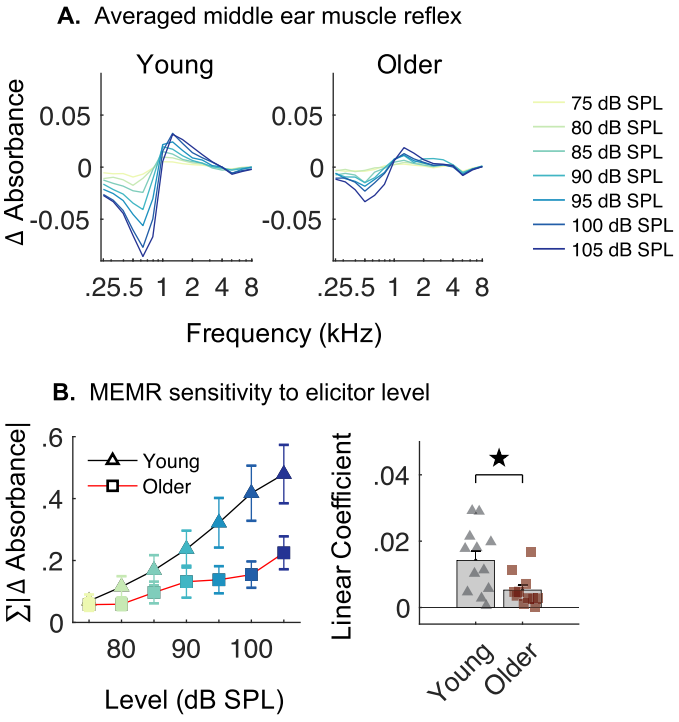

Fig. 2. A) Mean MEMR responses for levels 75–105 dB SPL for young and older participants. B) Sum of absolute change in absorbance over frequency for levels 75–105 dB SPL for young and older participants (left), and the slope of the linear fit of the growth level function for each participant (right). Error bars show SEM. $\star = p < 0.05$, $\star\star = p < 0.01$, $\star\star\star = p < 0.001$.

The younger listeners showed larger MEMR responses than the older listeners at higher noise elicitor levels. This is also reflected in the left panel of Fig. 2B) which shows the sum of absolute change in absorbance as a function of level, averaged across frequency, for the younger listeners (triangles) and the older listeners (squares). The right panel of Fig. 2B) shows the slope of the linear functions fitted to level growth functions of the two listener groups. The younger listeners showed significantly steeper slopes than the older listeners ($t(21) = 2.7330$, $p = 0.0118$), indicating a reduced strength of the MEMR at higher elicitor levels in the older group. However, even though the MEMR values were larger among the younger listeners, a large variability between the individual participants was found, consistent with results from previous work (Guest et al., 2019).

3.3. Effects of age on frequency sweep FFRs

To investigate effects of age on phase-locked neural activity across a range of frequencies, we first considered FFRs to continuous frequency sweeps. Fig. 3A) shows the spectrogram of the cosine sweep stimulus, sweeping continuously between 200 Hz and 1200 Hz. Fig. 3B) shows the average FFR responses to the sweep stimulus for the young (left) and the older (right) listeners. As a global similarity metric across frequency and time, the cross-correlation between the time-domain EEG response and the sweep stimulus was computed. Fig. 3C) shows the cross-correlation coefficient for the young (triangles) and the older listeners (squares). The analysis suggests a significantly reduced response to the sweep stimulus in the older listeners ($t(22) = 3.0526$, $p = 0.0063$). To quantify the differences in the FFR between the groups at the different frequencies in the sweep, the FFR spectral amplitudes were extracted and subjected to statistical permutation tests (see Meth-

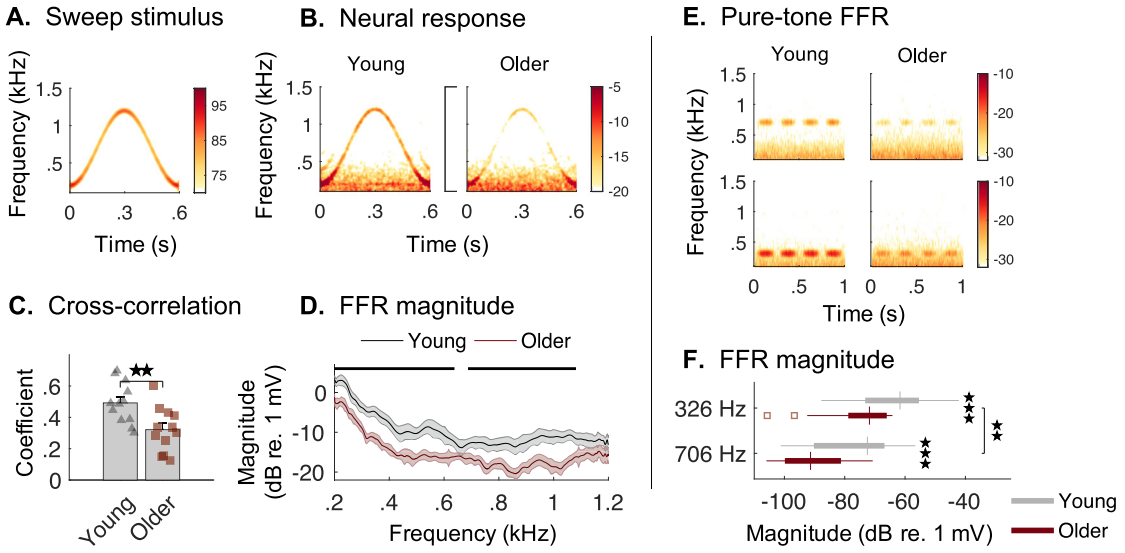

Fig. 3. FFR results. A) Spectrogram representation of the sinusoidal sweep stimulus. Color bar indicates presented sound pressure level (dB). B) Spectrograms of FFR responses to the sweep stimulus in the young (left) and older (right) listener groups. Color bars indicate EEG magnitude (dB re. 1 mV). C) Average cross-correlation coefficients in young and older listeners. D) FFR magnitudes at time-frequency bins of the sweep stimulation for young and older listeners. Shaded error bars represent +/- 1 SEM. Solid black lines above the curves indicate significant differences between listener groups after false discovery rate correction. E) Spectrograms of FFR responses to pure-tones at 706 Hz (top) and 326 Hz (bottom) for young (left) and older (right) listeners. F) Box plot of FFR magnitudes for 326 Hz and 706 Hz pure-tone stimuli for young and older listeners. Unfilled squares indicates non-significant data points compared to the noise floor. Error bars show SEM. $\star$=$p < 0.05$, $\star\star$ =$p < 0.01$, $\star\star\star$ =$p < 0.001$.

ods). Repeated measures across frequencies was accounted for using false discovery rate. Fig. 3D) shows the FFR amplitudes as a function of frequency for both listener groups. The FFR amplitudes were consistently smaller in amplitude across frequency in the older listeners than in the younger listeners. Frequency regions with significantly reduced FFR responses in the older group (black lines in Fig. 3D) were identified both at lower (200–600 Hz) and higher frequencies (700–1100 Hz).

3.4. Effects of age on pure-tone FFRs

The FFR responses to the sweep stimuli indicated reduced neural phase-locking in the older listeners at both lower and higher frequencies. Age-related changes could relate to the dynamic nature of the sweep stimulation (Clinard and Cotter, 2015). We therefore investigated FFR responses to pure tones separately at a lower (326 Hz) and a middle frequency (706 Hz) in the two listener groups. Fig. 3E) shows spectrograms of the group averaged EEG responses to the 706 Hz tone (top panels) and the 326 Hz tone (bottom panels) for the two listener groups. The FFR responses were quantified in terms of the spectral amplitudes at the stimulation frequency. Fig. 3F) shows group-based FFR amplitude boxplots for the young (gray bars) and the older listeners (red bars). All listeners showed significant responses to both stimuli, except for two of the older listeners where no significant FFR response could be obtained to the lower-frequency tone (unfilled squares). Compared to the young listeners, the older listeners showed significantly reduced FFR responses at both stimulation frequencies (ANOVA main effect of age: $F(1,44) = 17.3062$, $p < 0.001$). Additionally, the FFRs to the lower-frequency tone (326 Hz) were significantly larger than those to the higher-frequency tone in both listener groups (ANOVA, main effect of frequency: $F(1,44) = 9.0473$, $p = 0.0098$). No significant interactions between frequency and age were found. In agreement with these observations, the stimulus-response cross-correlation analysis showed similar effects of age and frequency (ANOVA main effect of age: $F(1,44) = 22.6711$, $p < 0.001$; main effect of frequency $F(1,44) = 11.7565$, $p = 0.0035$). Fig. 4 shows the

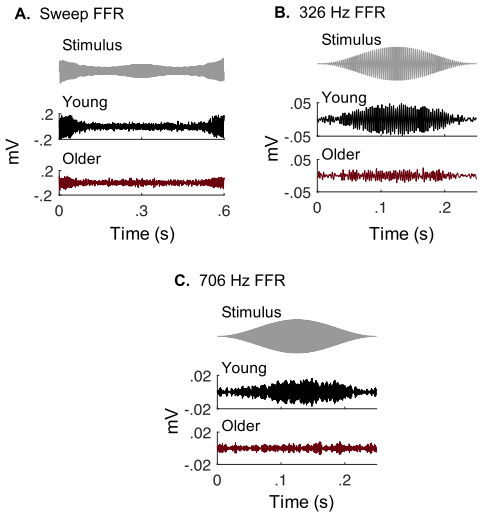

Fig. 4. Grand average time-domain FFRs. Averaged FFR for A) sweep stimulus, B) 326 Hz pure-tone, and C) 706 Hz pure-tone. In all panels, stimuli are shown in gray, and averaged FFRs are shown in black for young and red for older listeners. Pure-tone FFRs (B and C) have been bandpass filtered +/- 100 Hz around the stimulus frequency for visualization purposes.

average time-domain FFR to both sweeps and pure-tone stimuli for both listener groups.

To ensure that differences between the two groups were not a result of a different quality of the EEG recordings, we also calculated the SNR between the FFR and the surrounding noise floor. No differences between groups were found in terms of the noise floor level ($F(1,44) = 0.0043$, $p = 0.9475$). FFRs with and without the presence of the contralateral noise masker revealed no significant difference in FFR amplitudes for young (Bonferroni corrected $p < 0.0125$: 326 Hz: $t(11) = 2.7668$, $p = 0.0231$, 706Hz: $t(11) = 1.9310$, $p = 0.0676$) or for older listeners (326 Hz: $t(11) = 1.1292$, $p = 0.3090$, 706 Hz: $t(11) = -1.9736$, $p = 0.0760$), suggesting no effect of efferent feedback on the FFR.

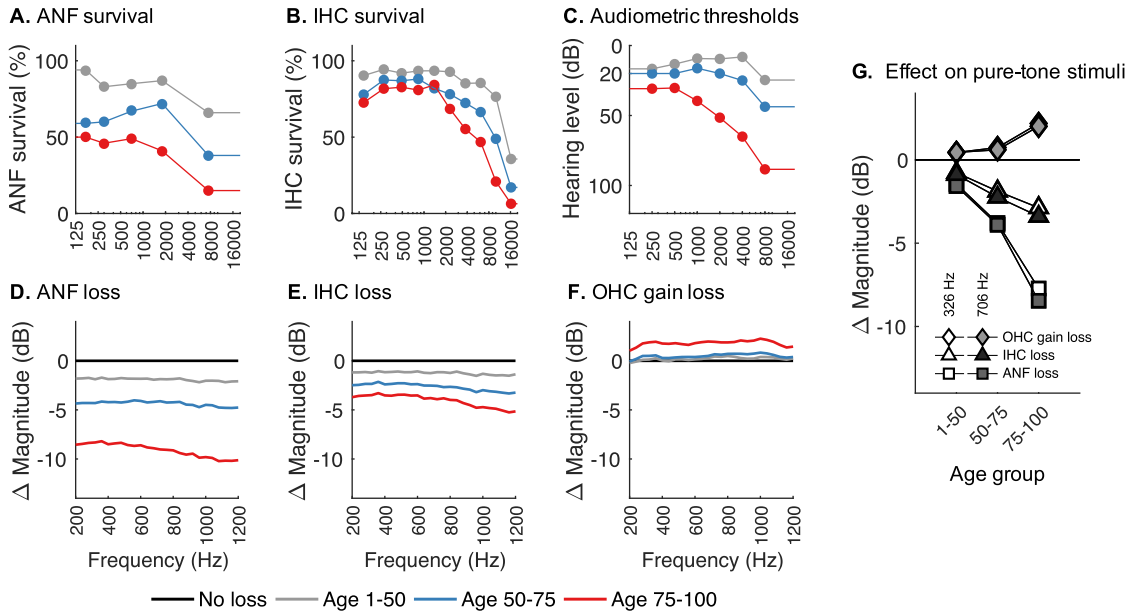

Fig. 5. Model-generated AN frequency-following responses to the sweep and pure tone stimuli (D-G) for different levels cochlear degeneration (A-B) and hearing loss (C) in aging humans. A) Mean ANF survival from human temporal bone histopathology (Wu et al., 2020) for three age groups. Losses are expressed in% of survival as a function of cochlear frequency. B) Mean IHC survival. C) Mean audiometric thresholds, D) Effect of ANF loss on the change in AN response to the sweep relative to the unimpaired model. D) Effect of IHC loss on the AN response. F) Effect of OHC gain loss corresponding to audiometric threshold shifts on AN responses. G) Change in AN responses to pure tones at 326 Hz (white) and 705 Hz (shaded) with OHC gain loss (diamonds), IHC deafferentation (triangles) or ANF loss (squares).

3.5. Auditory nerve modeling

We used a computational model of the auditory nerve (Bruce et al., 2018) to examine the effects of age-related hair-cell and AN degeneration. The modeling allowed us to dissociate effects of hair cell loss from neural degeneration on AN responses to the tone stimuli used in the current FFR experiments. We did not attempt to simulate the FFR generated in the central auditory brainstem (Dau, 2003; Rønne et al., 2012; Verhulst et al., 2018). Rather, assuming that the stimulus representation at the level of the nerve is a bottleneck for subsequent neural processing (Joris et al., 2004), we used the model to investigate whether age-related AN degeneration was qualitatively consistent with age effects observed in the FFR.

To model age-related degeneration, we used histopathological data from human temporal bones that quantified hair-cell and ANF survival in aging humans (Wu et al., 2020). Fig.5A and B shows the mean ANF and IHC fractional survival for all 120 cases divided into three age groups, and Fig. 5C shows their mean hearing loss. In the model, we separately removed ANFs or IHCs corresponding to the histological data for each age group and examined AN responses to the sweep stimuli used in the FFR experiments (see methods). Fig. 5D and 5E shows the effect of age-related loss of ANFs and IHCs, respectively, on the change in magnitude of the summed phase-locked AN response relative to an intact 'unimpaired' model. ANF loss in older subjects was found to strongly reduce frequency-following AN activity. Importantly, the phase-locked AN response was uniformly reduced across frequency, consistent with the age effects observed in the FFR data. Noticeably, the reduction was substantial already in the 50–75 years age group where thresholds were relatively normal (Fig. 5C) up to 4 kHz. However, IHC loss, although present mostly in the basal part of the cochlea, also led to a uniform reduction of the phase-locked AN response at lower frequencies, even though this effect was markedly smaller than for ANF loss.

OHC dysfunction cannot directly be modelled from the histology data, which quantifies only cell survival, because the relation between OHC loss and changes in the amplifier gain is not known. Instead, to examine the effects of OHC dysfunction we reduced the OHC gain, as implemented in Bruce et al. (2003), in proportion to the audiometric thresholds of the subjects (Fig. 5C). Loss of OHC gain did *not* reduce the phase-locked AN response to sweeps (Fig. 5F). To further investigate age-related hearing loss, we used age-normal audiometric profiles from a large sample (Rodríguez Valiente et al., 2014) where narrower age groups were defined and audiometric frequencies up to 20 kHz were measured (Fig. 6A). Again, in the framework of the model, even large degrees of OHC gain loss at high frequencies did not reduce the phase-locked AN response to the sweep stimulus (Fig. 6B).

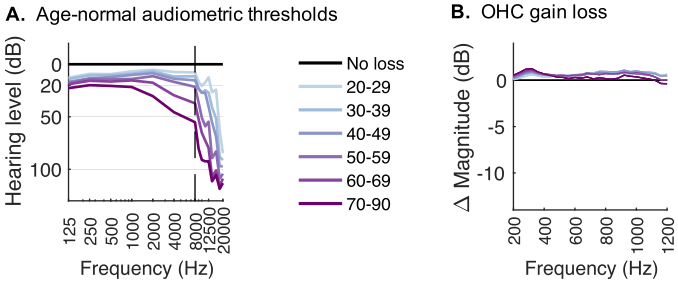

Fig. 6. A) Age-normal sensitivity curves replotted from (Rodríguez Valiente et al., 2014). Each curve represents the mean hearing threshold in dB HL for six different age groups. B) Relative magnitude change due to sensitivity loss attributed OHC gain loss in the sweep stimulus for the six mean age group sensitivity profiles seen in A.

Simulated AN responses were also obtained using the two pure-tone stimuli used in the FFR experiment. Fig. 5G shows the change in magnitude of the simulated phase-locked AN response for each age group and for the different types of cochlear impairment. Again, the greatest reduction was observed with loss of ANFs (Fig. 5G, squares), similar to the effects obtained for the sweep stimulus. The reduction was virtually identical at 326 Hz and 706 Hz, confirming a relatively broadband reduction as ob-

served with the sweep stimulus. A small increase was found in the case of OHC dysfunction (Fig. 5G, diamonds), most likely due to the loss of cochlear compressive gain.

4. Discussion

Consistent with previous work, our study confirmed that pure-tone FFRs are reduced in older human listeners with clinically normal hearing thresholds. We also found that this age-related reduction occurs across stimulus frequencies in the range examined (200–1200 Hz). Using model simulations, we found this reduction across frequencies to be qualitatively consistent with the pattern of age-related degeneration of ANFs suggested by human inner ear histopathology. Model simulations also indicated that OHC dysfunction, if present, would have little or no impact on the phase-locked population response at the level of the AN (cf. Encina-Llamas et al. (2019, 2021)). If the AN neurophonic response is assumed to be a bottleneck on the downstream synchronous neural activity reflected in the FFR (Dau, 2003), then peripheral degeneration may contribute significantly to the response reduction seen in the experimental data. If the FFR is selectively sensitive to cochlear neural degeneration and not affected by OHC status, then this may also imply a clinical potential of the FFR, also in listeners with hearing loss. However, simulations also indicated that high-frequency loss of IHCs may reduce the amount of phase-locking at lower frequencies, albeit to a lesser degree.

In contrast to our findings, some previous studies reported reduced FFR amplitudes in normal-hearing older adults predominantly at higher frequencies (1000 Hz), but not at lower ones (500 Hz, Clinard et al., 2010; Grose et al., 2017). However, age-related reductions have also been observed previously at lower frequencies (~400 Hz) with frequency sweeps as in the current study (Clinard and Cotter, 2015). Clinard and Cotter (2015) argued that this effect may be specific to dynamic frequency content (such as sweeps), reflecting degraded processing of time-varying spectral cues in the aging auditory system. Yet, in the current study, FFR responses to pure tones were found to be reduced also at lower frequencies (326 Hz). Consistent with this, reduced FFRs to the fundamental frequency (F0) of sustained vowel sounds, i.e. evoked by lower frequencies, have also been frequently reported (e.g. Anderson et al., 2012; Presacco et al., 2016; Roque et al., 2019).

Reduced FFR responses in older listeners with clinically normal audiograms have been argued to indicate a degradation of temporal processing originating in the central auditory system (Anderson et al., 2012; Clinard and Cotter, 2015; Clinard and Tremblay, 2013). However, hearing thresholds in the clinically normal range are not sufficient to rule out a peripheral origin of these FFR changes. Loss of AN fibers, by itself, has only a minor effect on audiometric thresholds (Schuknecht and Woellner, 1955; Wu et al., 2020). In the current study, we included other measures that could indicate peripheral degeneration in our clinically normal-hearing listeners. Although the older subjects had clinically normal hearing at standard audiometric frequencies up to 6 kHz, thresholds at the extended high frequencies (> 8 kHz) were found to be distinctly elevated. Additionally, MEMR level-growth functions were significantly reduced in the older group. Elevated high-frequency thresholds and reduced MEMRs may indicate peripheral degeneration beyond what is indicated by the clinical audiogram (Bharadwaj et al., 2019; Liberman et al., 2016; Mepani et al., 2019; Valero et al., 2016). It is likely that most older listeners with clinically normal thresholds have high-frequency threshold loss similar to that seen here (Matthews et al., 1997). A peripheral source of the FFR reduction in older listeners cannot be excluded without other measures of peripheral function. Indeed, identifying older listeners with a peripheral hearing status matching that of young listeners may be challenging. A larger sample size than the one used here might further explore the relation between the FFR and measures of peripheral hearing status.

Direct evidence for effects of age-related AN degeneration on scalp-recorded FFRs is missing. It is well-established that AN damage reduces the neurophonic response recorded close to the nerve (Choudhury et al., 2012; Fontenot et al., 2017; Henry, 1995; Snyder and Schreiner, 1984), but evidence about the consequences on scalp-recorded FFRs is sparse. Envelope-following responses (EFRs), on the other hand, have been used more extensively to examine the functional consequences of cochlear synaptopathy. Similar to FFR responses to tone carriers, the scalp-recorded EFR to amplitude modulated (AM) stimuli is thought to reflect population phase-locked activity which may be reduced by AN damage. In rodents, EFRs to modulation frequencies around 1 kHz are dominated by AN activity and are reduced with synaptopathy following noise exposure (Shaheen et al., 2015) or aging (Parthasarathy et al., 2018, 2016, 2014). The magnitude of EFR reductions around 1 kHz has been shown to predict the degree of ANF loss, i.e. the percentage of surviving fibers (Shaheen et al., 2015), also before age-related loss of thresholds emerge (Parthasarathy et al., 2019; Parthasarathy and Kujawa, 2018). In humans, age-related EFR reductions have been observed at modulation frequencies around 120 Hz where the response is dominated by subcortical generators (Vasilkov et al., 2021). Human EFRs at lower modulation frequencies are increasingly dominated by cortical sources (Herdman et al., 2002), and lower modulation frequencies show minimal effects or are even enhanced with age (Goossens et al., 2016, 2018; Grose et al., 2009; Herrmann et al., 2017; Lai et al., 2017; Parthasarathy and Bartlett, 2012). This could be explained by the presence of a central gain enhancement mechanism that restores sound-evoked response levels after ANF loss but not precise temporal coding (Chambers et al., 2016; Herrmann et al., 2017; Parthasarathy et al., 2014). It is therefore unclear whether EFR enhancements at lower modulation frequencies occur because such gain mechanisms mostly affect slower neural activity or because of a stronger contribution from more central sources in the EFR (or a combination of both). It is, perhaps, less likely that FFR responses to temporal fine structure are similarly affected by central compensation mechanisms (Parthasarathy and Kujawa, 2018). More generally, it remains unclear whether the population responses to envelope and fine-structure are similarly limited by the number of contributing AN fibers (Joris and Smith, 2008).

It is important to highlight that the FFR represents a population response. Single AN fibers that survive degeneration in aged animals can retain intact coding of both temporal fine structure and envelope (Heeringa et al., 2020). Accordingly, in our model simulations, we simulated AN degeneration by removing a percentage of fibers while leaving the remaining fibers functionally intact. AN phase-locking computed from the summed activity across remaining fibers decreased as the number of AN fibers was reduced. However, the generation of a synchronous population response is most likely not the result of a simple summation at the level of the AN. Convergence of multiple AN fibers at their target synapse is known to enhance phase-locking to the fine-structure of low frequency tones (<1 kHz) in CN bushy neurons relative to the AN (Joris et al., 1994a, 1994b). Such synchronization enhancement in the brainstem has been proposed to rely on a synaptic mechanism that requires coincident AN inputs for spike generation (Chanda and Xu-Friedman, 2010; Kuhlmann et al., 2002; Rothman and Young, 1996) which effectively reduces the variability in spike-timing in the AN (Joris and Smith, 2008; Xu-Friedman and Regehr, 2005). Importantly, synchronization strength at the postsynaptic output increases with the number of converging ANF inputs (Xu-Friedman and Regehr, 2005). The effects of ANF loss might therefore be particularly pronounced post-synaptically where a reduction in the ANF population size would reduce this synchrony

enhancement occurring for low-frequency tones (<1 kHz). This is consistent with the age-related FFR reductions at lower frequencies (<1 kHz) observed in the current study. Since the FFR reflects phase-locking at the brainstem level, FFR reductions at lower frequencies may thus be the consequence of ANF loss observed post-synaptically. Yet, the model framework used in the current study does not incorporate synaptic mechanisms that account for any synchronization enhancement, and including these may yield a better estimation of the effects of ANF loss on synchronous activity at the brainstem level.

4.1. Concluding comments

The current study offers a peripheral account of FFR reductions in older listeners. Recent human temporal bone histopathology indicates that AN fibers are vulnerable to aging and that cochlear neural degeneration may precede hearing threshold loss and typically exceeds the loss of sensory cells (Wu et al., 2020, 2019). Bearing this in mind, we reasoned that older listeners with normal thresholds would, on average, have a higher degree of ANF loss compared to young normal-hearing listeners. Reduced FFRs in older listeners is consistent with a reduced number of ANFs contributing to the population synchronous response. FFR reductions were observed across stimulation frequency (200–1200 Hz), as would be expected from a reduction in the number of ANFs, whereas a centrally induced age-dependent reduction in temporal precision (Frisina, 2001) would be expected to reduce responses more at higher frequencies (Clinard et al., 2010; Clinard and Cotter, 2015). Yet, without more direct evidence about the AN status in our older normal-hearing subjects, we cannot rule out that age-related changes occurring in the central auditory system also contribute significantly to the reduced FFR. It remains uncertain how AN degeneration translates to more central stages where the scalp-recorded FFR is generated, and evidence about how central stages adapt to neural degeneration in the auditory periphery is critically missing. Yet, if AN degeneration is indeed sensitive to the response synchrony represented by the FFR, as we propose, then the FFR may provide valuable diagnostic information .

Declaration of Competing Interest

The authors declare no competing financial interests.

CRediT authorship contribution statement

Jonatan Märcher-Rørsted: Conceptualization, Methodology, Software, Formal analysis, Data curation, Investigation, Writing – original draft, Visualization, Project administration. **Gerard Encina-Llamas:** Conceptualization, Methodology, Software, Formal analysis, Supervision, Writing – review & editing. **Torsten Dau:** Conceptualization, Supervision, Project administration, Writing – review & editing, Funding acquisition. **M. Charles Liberman:** Conceptualization, Resources, Writing – review & editing. **Pei-zhe Wu:** Resources, Investigation, Writing – review & editing. **Jens Hjortkjær:** Conceptualization, Methodology, Formal analysis, Investigation, Writing – original draft, Supervision, Project administration, Funding acquisition.

Acknowledgments

This work was supported by the Novo Nordisk Foundation synergy grant NNF17OC0027872 (UHeal) and a grant from the National Institutes of Health (P50 DC015857).

References

Abdala, C., Folsom, R.C., 1995. Frequency contribution to the click-evoked auditory brain-stem response in human adults and infants. J. Acoust. Soc. Am. 97, 2394–2404. doi:10.1121/1.411961.

Anderson, S., Parbery-Clark, A., White-Schwoch, T., Kraus, N., 2012. Aging affects neural precision of speech encoding. J. Neurosci. 32, 14156–14164. doi:10.1523/jneurosci.2176-12.2012.

Benjamini, Y., Hochberg, Y., 1995. Controlling the false discovery rate : a practical and powerful approach to multiple testing. Society 57, 289–300.

Bharadwaj, H.M., Mai, A.R., Simpson, J.M., Choi, I., Heinz, M.G., Shinn-Cunningham, B.G., 2019. Non-invasive assays of cochlear synaptopathy – candidates and considerations. Neuroscience 407, 53–66. doi:10.1016/j.neuroscience.2019.02.031.

Bidelman, G.M., 2018. Subcortical sources dominate the neuroelectric auditory frequency-following response to speech. Neuroimage 175, 56–69. doi:10.1016/j.neuroimage.2018.03.060.

Bidelman, G.M., Villafuerte, J.W., Moreno, S., Alain, C., 2014. Age-related changes in the subcortical-cortical encoding and categorical perception of speech. Neurobiol. Aging 35, 2526–2540. doi:10.1016/j.neurobiolaging.2014.05.006.

Bruce, I.C., Erfani, Y., Zilany, M.S.A., 2018. A phenomenological model of the synapse between the inner hair cell and auditory nerve: implications of limited neurotransmitter release sites. Hear. Res. 360, 40–54. doi:10.1016/j.heares.2017.12.016.

Bruce, I.C., Sachs, M.B., Young, E.D., 2003. An auditory-periphery model of the effects of acoustic trauma on auditory nerve responses. J. Acoust. Soc. Am. 113, 369–388. doi:10.1121/1.1519544.

Chambers, A.R., Resnik, J., Yuan, Y., Whitton, J.P., Edge, A.S., Liberman, M.C., Polley, D.B., 2016. Central gain restores auditory processing following near-complete cochlear denervation. Neuron 89, 867–879. doi:10.1016/j.neuron.2015.12.041.

Chanda, S., Xu-Friedman, M.A., 2010. A low-affinity antagonist reveals saturation and desensitization in mature synapses in the auditory brain stem. J. Neurophysiol. 103, 1915–1926. doi:10.1152/jn.00751.2009.

Choudhury, B., Fitzpatrick, D.C., Buchman, C.A., Wei, B.P., Dillon, M.T., He, S., Adunka, O.F., 2012. Intraoperative round window recordings to acoustic stimuli from cochlear implant patients. Otol. Neurotol. 33, 1507–1515. doi:10.1097/MAO.0b013e31826dbc80.

Clinard, C.G., Cotter, C.M., 2015. Neural representation of dynamic frequency is degraded in older adults. Hear. Res. 323, 91–98. doi:10.1016/j.heares.2015.02.002.

Clinard, C.G., Tremblay, K.L., 2013. Aging degrades the neural encoding of simple and complex sounds in the human brainstem. J. Am. Acad. Audiol. 24, 590–599. doi:10.3766/jaaa.24.7.7.

Clinard, C.G., Tremblay, K.L., Krishnan, A.R., 2010. Aging alters the perception and physiological representation of frequency: evidence from human frequency-following response recordings. Hear. Res. 264, 48–55. doi:10.1016/j.heares.2009.11.010.

Dau, T., 2003. The importance of cochlear processing for the formation of auditory brainstem and frequency following responses. J. Acoust. Soc. Am. 113, 936–950. doi:10.1121/1.1534833.

Dobie, R.A., Wilson, M.J., 1996. A comparison of t-test, F test, and coherence methods of detecting steady-state auditory-evoked potentials, distortion-product otoacoustic emissions, or other sinusoids 100, 2236–2246.

Encina-Llamas, G., Dau, T., Epp, B., 2021. On the use of envelope following responses to estimate peripheral level compression in the auditory system. Sci. Rep. 11, 6962. doi:10.1038/s41598-021-85850-x.

Encina-Llamas, G., Harte, J.M., Dau, T., Shinn-Cunningham, B., Epp, B., 2019. Investigating the effect of cochlear synaptopathy on envelope following responses using a model of the auditory nerve. JARO - J. Assoc. Res. Otolaryngol. 20, 363–382. doi:10.1007/s10162-019-00721-7.

Fernandez, K.A., Jeffers, P.W.C., Lall, K., Liberman, M.C., Kujawa, S.G., 2015. Aging after noise exposure: acceleration of cochlear synaptopathy in “recovered” ears. J. Neurosci. 35, 7509–7520. doi:10.1523/JNEUROSCI.5138-14.2015.

Fontenot, T.E., Giardina, C.K., Fitzpatrick, D.C., 2017. A model-based approach for separating the cochlear microphonic from the auditory nerve neurophonic in the ongoing response using electrocochleography. Front. Neurosci. 11, 1–18. doi:10.3389/fnins.2017.00592.

Frisina, R.D., 2001. Subcortical neural coding mechanisms for auditory temporal processing. Hear. Res 158, 1–27. doi:10.1016/S0378-5955(01)00296-9.

Frisina, R.D., Frisina, R.D., 1997. Speech recognition in noise and presbycusis: relations to possible neural mechanisms. Hear. Res. 106, 95–104. doi:10.1016/S0378-5955(97)00006-3.

Fu, Z., Yang, H., Chen, F., Wu, X., Chen, J., 2019. Brainstem encoding of frequency-modulated sweeps is relevant to Mandarin concurrent-vowels identification for normal-hearing and hearing-impaired listeners. Hear. Res. 380, 123–136. doi:10.1016/j.heares.2019.06.005.

Gleich, O., Semmler, P., Strutz, J., 2016. Behavioral auditory thresholds and loss of ribbon synapses at inner hair cells in aged gerbils. Exp. Gerontol. 84, 61–70. doi:10.1016/j.exger.2016.08.011.

Goossens, T., Vercammen, C., Wouters, J., van Wieringen, A., 2016. Aging affects neural synchronization to speech-related acoustic modulations. Front. Aging Neurosci. 8, 1–16. doi:10.3389/fnagi.2016.00133.

Goossens, T., Vercammen, C., Wouters, J., van Wieringen, A., 2018. Neural envelope encoding predicts speech perception performance for normal-hearing and hearing-impaired adults. Hear. Res. 370, 189–200. doi:10.1016/j.heares.2018.07.012.

Grose, J.H., Buss, E., Hall, J.W., 2017. Loud music exposure and cochlear synaptopathy in young adults: isolated auditory brainstem response effects but no perceptual consequences. Trends Hear doi:10.1177/2331216517737417.

Grose, J.H., Mamo, S.K., Hall, J.W., 2009. Age effects in temporal envelope processing: speech unmasking and auditory steady state responses. Ear Hear 30, 568–575. doi:10.1097/AUD.0b013e3181ac128f.

Guest, H., Munro, K.J., Plack, C.J., 2019. Acoustic middle-ear-muscle-reflex thresholds in humans with normal audiograms: no relations to tinnitus, speech perception in noise, or noise exposure. Neuroscience 1–8 https://doi.org/S0306452218308285.

Heeringa, A.N., Zhang, L., Ashida, G., Beutelmann, R., Steenken, F., Köppl, C., 2020. Temporal coding of single auditory nerve fibers is not degraded in aging gerbils. J. Neurosci. 40, 343–354. doi:10.1523/JNEUROSCI.2784-18.2019.

Henry, K.R., 1995. Auditory nerve neurophonic recorded from the round window of the Mongolian gerbil. Hear. Res. 90, 176–184. doi:10.1016/0378-5955(95)00162-6.

Herdman, A.T., Lins, O., Van Roon, P., Stapells, D.R., Scherg, M., Picton, T.W., 2002. Intracerebral sources of human auditory steady-state responses. Brain Topogr 15, 69–86. doi:10.1023/A:1021470822922.

Herrmann, B., Parthasarathy, A., Bartlett, E.L., 2017. Ageing affects dual encoding of periodicity and envelope shape in rat inferior colliculus neurons. Eur. J. Neurosci. 45, 299–311. doi:10.1111/ejn.13463.

Humes, L.E., 2005. Do "auditory processing" tests measure auditory processing in the elderly? Ear Hear 26, 109–119. doi:10.1097/00003446-200504000-00001.

John, M.S., Dimitrijevic, A., Picton, T.W., 2001. Weighted averaging of steady-state responses. Clin. Neurophysiol. 112, 555–562. doi:10.1016/S1388-2457(01)00456-4.

Joris, P.X., Carney, L.H., Smith, P.H., Yin, T.C.T., 1994a. Enhancement of neural synchronization in the anteroventral cochlear nucleus. I. Responses to tones at the characteristic frequency. J. Neurophysiol. 71, 1022–1036. doi:10.1152/jn.1994.71.3.1022.

Joris, P.X., Schreiner, C.E., Rees, A., 2004. Neural processing of amplitude-modulated sounds. Physiol. Rev. 84, 541–577. doi:10.1152/physrev.00029.2003.

Joris, P.X., Smith, P.H., 2008. The volley theory and the spherical cell puzzle. Neuroscience 154, 65–76. doi:10.1016/j.neuroscience.2008.03.002.

Joris, P.X., Smith, P.H., Yin, T.C.T., 1994b. Enhancement of neural synchronization in the anteroventral cochlear nucleus. II. Responses in the tuning curve tail. J. Neurophysiol. 71, 1037–1051. doi:10.1152/jn.1994.71.3.1037.

Keithley, E.M., Ryan, A.F., Woolf, N.K., 1989. Spiral ganglion cell density in young and old gerbils. Hear. Res. 38, 125–133. doi:10.1016/0378-5955(89)90134-2.

Kraus, N., Skoe, E., 2010. Auditory brainstem response to complex sounds: a tutorial. Ear Hear 31, 302–324. doi:10.1097/AUD.0b013e3181cdb272.

Krishnan, A., 2006. Human frequency following response. Audit. evoked potentials Basic Princ. Clin. Appl. 313–315.

Kuhlmann, L., Burkitt, A.N., Paolini, A., Clark, G.M., 2002. Summation of spatiotemporal input patterns in leaky integrate-and-fire neurons: application to neurons in the cochlear nucleus receiving converging auditory nerve fiber input. J. Comput. Neurosci. 12, 55–73. doi:10.1023/A:1014994113776.

Kujawa, S.G., Liberman, M.C., 2009. Adding Insult to Injury: cochlear nerve degeneration after 29, 14077–14085. https://doi.org/10.1523/JNEUROSCI.2845-09.2009.Adding

Lai, J., Sommer, A.L., Bartlett, E.L., 2017. Age-related changes in envelope-following responses at equalized peripheral or central activation. Neurobiol. Aging 58, 191–200. doi:10.1016/j.neurobiolaging.2017.06.013.

Liberman, M.C., 1978. Auditory-nerve response from cats raised in a low-noise chamber. J. Acoust. Soc. Am. 63, 442–455. doi:10.1121/1.381736.

Liberman, M.C., Epstein, M.J., Cleveland, S.S., Wang, H., Maison, S.F., 2016. Toward a differential diagnosis of hidden hearing loss in humans. PLoS ONE 11, 1–15. doi:10.1371/journal.pone.0162726.

Mamo, S.K., Grose, J.H., Buss, E., 2016. Speech-evoked ABR: effects of age and simulated neural temporal jitter. Hear. Res. 333, 201–209. doi:10.1016/j.heares.2015.09.005.

Marmel, F., Linley, D., Carlyon, R.P., Gockel, H.E., Hopkins, K., Plack, C.J., 2013. Subcortical neural synchrony and absolute thresholds predict frequency discrimination independently. JARO - J. Assoc. Res. Otolaryngol. 14, 757–766. doi:10.1007/s10162-013-0402-3.

Marsh, J.T., Brown, W.S., Smith, J.C., 1974. Differential brainstem pathways for the conduction of auditory frequency-following responses. Electroencephalogr. Clin. Neurophysiol. 36, 415–424. doi:10.1016/0013-4694(74)90192-8.

Matthews, L.J., Lee, F.-.S., Mills, J.H., Dubno, J.R., 1997. Extended high-frequency thresholds in older adults. J. Speech, Lang. Hear. Res. 40, 208–214. doi:10.1044/jslhr.4001.208.

Mepani, A.M., Kirk, S.A., Hancock, K.E., Bennett, K., de Gruttola, V., Liberman, M.C., Maison, S.F., 2019. Middle ear muscle reflex and word recognition in "normal-hearing" adults. Ear Hear 1. doi:10.1097/aud.0000000000000804.

Parthasarathy, A., Bartlett, E., 2012. Two-channel recording of auditory-evoked potentials to detect age-related deficits in temporal processing. Hear. Res. 289, 52–62. doi:10.1016/j.heares.2012.04.014.

Parthasarathy, A., Datta, J., Torres, J.A.L., Hopkins, C., Bartlett, E.L., 2014. Age-related changes in the relationship between auditory brainstem responses and envelope-following responses. JARO - J. Assoc. Res. Otolaryngol. 15, 649–661. doi:10.1007/s10162-014-0460-1.

Parthasarathy, A., Hancock, K.E., Bennett, K., DeGruttola, V., Polley, D.B., 2019. Neural signatures of disordered multi-talker speech perception in adults with normal hearing. bioRxiv 1–22. doi:10.1101/744813.

Parthasarathy, A., Herrmann, B., Bartlett, E.L., 2018. Aging alters envelope representations of speech-like sounds in the inferior colliculus. bioRxiv, 266650 doi:10.1101/266650.

Parthasarathy, A., Kujawa, S.G., 2018. Synaptopathy in the aging cochlea: characterizing early-neural deficits in auditory temporal envelope processing. J. Neurosci. 38, 7108–7119. doi:10.1523/JNEUROSCI.3240-17.2018.

Parthasarathy, A., Lai, J., Bartlett, E.L., 2016. Age-related changes in processing simultaneous amplitude modulated sounds assessed using envelope following responses. JARO - J. Assoc. Res. Otolaryngol. 17, 119–132. doi:10.1007/s10162-016-0554-z.

Pichora-Fuller, M.K., Schneider, B.A., MacDonald, E., Pass, H.E., Brown, S., 2007. Temporal jitter disrupts speech intelligibility: a simulation of auditory aging. Hear. Res. 223, 114–121. doi:10.1016/j.heares.2006.10.009.

Presacco, A., Simon, J.Z., Anderson, S., 2019. Speech-in-noise representation in the aging midbrain and cortex: effects of hearing loss. PLoS ONE 14, 1–26. doi:10.1371/journal.pone.0213899.

Presacco, A., Simon, J.Z., Anderson, S., 2016. Evidence of degraded representation of speech in noise, in the aging midbrain and cortex. J. Neurophysiol. 116, 2346–2355. doi:10.1152/jn.00372.2016.

Reale, R.A., Geisler, C.D., 1980. Auditory-nerve fiber encoding of two-tone approximations to steady-state vowels. J. Acoust. Soc. Am. 67, 891–902. doi:10.1121/1.383969.

Rodríguez Valiente, A., Trinidad, A., García Berrocal, J.R., Górriz, C., Ramírez Camacho, R., 2014. Extended high-frequency (9–20 kHz) audiometry reference thresholds in 645 healthy subjects. Int. J. Audiol. 53, 531–545. doi:10.3109/14992027.2014.893375.

Rønne, F.M., Dau, T., Harte, J., Elberling, C., 2012. Modeling auditory evoked brainstem responses to transient stimuli. J. Acoust. Soc. Am. 131, 3903–3913. doi:10.1121/1.3699171.

Roque, L., Gaskins, C., Gordon-Salant, S., Goupell, M.J., Andersona, S., 2019. Age effects on neural representation and perception of silence duration cues in speech. J. Speech, Lang. Hear. Res. 62, 1099–1116. doi:10.1044/2018_JSLHR-H-ASCC7-18-0076.

Rothman, J.S., Young, E.D., 1996. Enhancement of neural synchronization in computational models of ventral cochlear nucleus bushy cells. Audit. Neurosci. 2, 47–62.

Sachs, M.B., Voigt, H.F., Young, E.D., 1983. Auditory nerve representation of vowels in background noise. J. Neurophysiol. 50, 27–45. doi:10.1152/jn.1983.50.1.27.

Schuknecht, H.F., Woellner, R.C., 1955. An experimental and clinical study of deafness from lesions of the cochlear nerve. J. Laryngol. Otol. 69, 75–97. doi:10.1017/S0022215100050465.

Sergeyenko, Y., Lall, K., Liberman, M.C., Kujawa, S.G., 2013. Age-related cochlear synaptopathy: an early-onset contributor to auditory functional decline. J. Neurosci. 33, 13686–13694. doi:10.1523/JNEUROSCI.1783-13.2013.

Shaheen, L.A., Valero, M.D., Liberman, M.C., 2015. Towards a diagnosis of cochlear neuropathy with envelope following responses. JARO - J. Assoc. Res. Otolaryngol. 16, 727–745. doi:10.1007/s10162-015-0539-3.

Skoe, E., Krizman, J., Anderson, S., Kraus, N., 2015. Stability and plasticity of auditory brainstem function across the lifespan. Cereb. Cortex 25, 1415–1426. doi:10.1093/cercor/bht311.

Smith, J.C., Marsh, J.T., Brown, W.S., 1975. Far-field recorded frequency-following responses: evidence for the locus of brainstem sources. Electroencephalogr. Clin. Neurophysiol. 39, 465–472. doi:10.1016/0013-4694(75)90047-4.

Snyder, R.L., Schreiner, C.E., 1985. Forward masking of the auditory nerve neurophonic (ANN) and the frequency following response (FFR). Hear. Res. 20, 45–62. doi:10.1016/0378-5955(85)90058-9.

Snyder, R.L., Schreiner, C.E., 1984. The auditory neurophonic: basic properties. Hear. Res. 15, 261–280. doi:10.1016/0378-5955(84)90033-9.

Sohmer, H., Pratt, H., Kinarti, R., 1977. Sources of frequency following responses (FFR) in man. Electroencephalogr. Clin. Neurophysiol. 42, 656–664. doi:10.1016/0013-4694(77)90282-6.

Sun, X.-.M., 2012. Ear canal pressure variations versus negative middle ear pressure: comparison using distortion product otoacoustic emission measurement in humans. Ear Hear 33, 69–78. doi:10.1097/AUD.0b013e3182280326.

Suthakar, K., Liberman, M.C., 2021. Auditory-nerve responses in mice with noise-induced cochlear synaptopathy. J. Neurophysiol. doi:10.1152/jn.00342.2021.

Valero, M.D., Hancock, K.E., Liberman, M.C., 2016. The middle ear muscle reflex in the diagnosis of cochlear neuropathy. Hear. Res. 332, 29–38. doi:10.1016/j.heares.2015.11.005.

Vasilkov, V., Garrett, M., Mauermann, M., Verhulst, S., 2021. Enhancing the sensitivity of the envelope-following response for cochlear synaptopathy screening in humans: the role of stimulus envelope. Hear. Res. 400, 108132. doi:10.1016/j.heares.2020.108132.

Verhulst, S., Altoè, A., Vasilkov, V., 2018. Computational modeling of the human auditory periphery: auditory-nerve responses, evoked potentials and hearing loss. Hear. Res. 360, 55–75. doi:10.1016/j.heares.2017.12.018.

Verschooten, E., Joris, P.X., 2014. Estimation of neural phase locking from stimulus-evoked potentials. JARO - J. Assoc. Res. Otolaryngol. 15, 767–787. doi:10.1007/s10162-014-0465-9.

Viana, L.M., O'Malley, J.T., Burgess, B.J., Jones, D.D., Oliveira, C.A.C.P., Santos, F., Merchant, S.N., Liberman, L.D., Liberman, M.C., 2015. Cochlear neuropathy in human presbycusis: confocal analysis of hidden hearing loss in post-mortem tissue. Hear. Res. 327, 78–88. doi:10.1016/j.heares.2015.04.014.

Walton, J.P., 2010. Timing is everything: temporal processing deficits in the aged auditory brainstem. Hear. Res. 264, 63–69. doi:10.1016/j.heares.2010.03.002.

Worden, F.G., Marsh, J.T., 1968. Frequency-following (microphonic-like) neural responses evoked by sound. Electroencephalogr. Clin. Neurophysiol. 25, 42–52. doi:10.1016/0013-4694(68)90085-0.

Wu, P.Z., Liberman, L.D., Bennett, K., de Gruttola, V., O'Malley, J.T., Liberman, M.C., 2019. Primary neural degeneration in the human cochlea: evidence for hidden hearing loss in the aging ear. Neuroscience 407, 8–20. doi:10.1016/j.neuroscience.2018.07.053.

Wu, P.Z., O'Malley, J.T., de Gruttola, V., Charles Liberman, M., 2020. Age-related hearing loss is dominated by damage to inner ear sensory cells, not the cellular battery that powers them. J. Neurosci. 40, 6357–6366. doi:10.1523/JNEUROSCI.093720.2020.

Xu-Friedman, M.A., Regehr, W.G., 2005. Dynamic-clamp analysis of the effects of convergence on spike timing. II. Few synaptic inputs. J. Neurophysiol. 94, 2526–2534. doi:10.1152/jn.01308.2004.

Young, E.D., Sachs, M.B., 1979. Representation of steady-state vowels in the temporal aspects of the discharge patterns of populations of auditory-nerve fibers. J. Acoust. Soc. Am. 66, 1381–1403. doi:10.1121/1.383532.

Zilany, M.S.A., Bruce, I.C., Nelson, P.C., Carney, L.H., 2009. A phenomenological model of the synapse between the inner hair cell and auditory nerve: long-term adaptation with power-law dynamics. J. Acoust. Soc. Am. 126, 2390–2412. doi:10.1121/1.3238250.